Author's Post-print version. Article published in Applied Energy:
DOI: 10.1016/j.apenergy.2017.08.075
Published version: https://www.sciencedirect.com/science/article/pii/S0306261917310930

High temperature gasification of high heating-rate chars using a flat-flame reactor[1]

Tian Li[a,*], Yanqing Niu[b], Liang Wang[c], Christopher Shaddix[d], Terese Løvås[a]

[a]Department of Energy and Process Engineering, Faculty of Engineering, NTNU – Norwegian University of Science and Technology, Trondheim, Norway

[b] Key Laboratory of Thermo-Fluid Science and Engineering of MOE, School of Energy and Power Engineering, Xi'an Jiaotong University, Xi'an 710049, China

[c]SINTEF Energy Research, P.O. Box 4761, Sluppen, 7465 Trondheim, Norway

[d]Combustion Research Facility, Sandia National Laboratories, Livermore, California 94550, United States

*Corresponding author, E-mail address: tian.li@ntnu.no

Abstract:

The increasing interest in gasification and oxy-fuel combustion of biomass has heightened the need for a detailed understanding of char gasification in industrially relevant environments (i.e., high temperature and high-heating rate). Despite innumerable studies previously conducted on gasification of biomass, very few have focused on such conditions. Consequently, in this study the high-temperature gasification behavior of biomass-derived chars were investigated using non-intrusive techniques. Two biomass chars produced at a heating rate of approximately 10^4 K/s were subjected to two gasification environments and one oxidation environment in an entrained flow reactor equipped with an optical particle-sizing pyrometer. A coal char produced from a common U.S. low sulfur subbituminous coal was also studied for comparison. Both char and surrounding gas temperatures were precisely measured along the centerline of the furnace. Despite differences in the physical and chemical properties of the biomass chars, they exhibited rather similar reaction temperatures under all investigated conditions. On the other hand, a slightly lower particle temperature was observed in the case of coal char gasification, suggesting a higher gasification reactivity for the coal char. A comprehensive numerical model was applied to aid the understanding of the conversion of the investigated chars under gasification atmospheres. In addition, a sensitivity analysis was performed on the influence of four parameters (gas temperature, char diameter, char density, and steam concentration) on the carbon conversion rate. The results demonstrate that the gas temperature is the most important single variable influencing the gasification rate.

Keywords: Char, Biomass, Gasification, Particle temperature, Kinetics, Torrefaction

[1]A short version of the paper was presented at ICAE2016 on Oct 8-11, 2016, Beijing, China. This paper is a substantial extension of the conference paper.

Author's Post-print version. Article published in Applied Energy:
DOI: 10.1016/j.apenergy.2017.08.075
Published version: https://www.sciencedirect.com/science/article/pii/S0306261917310930

1. Introduction

Biomass is one of the most promising alternative energy sources due to its renewability. It is particularly attractive to convert biomass via gasification into syngas (which contains mainly H_2 and CO) as biomass-derived syngas can be used to sustainably produce liquid transportation fuels as well as important industrial chemical feedstocks such as lower olefins [1,2]. The gasification process, however, is very complex, especially the rate-limiting step of char conversion. The steam gasification reaction $C+H_2O \rightarrow CO+H_2$ and the Boudouard reaction $C+CO_2 \rightarrow 2CO$ heavily influence the overall product composition as well as the efficiency of the gasification process. In addition, during the combustion of biomass, char particles derived from the devolatilization step can also react with surrounding gases and be involved in gasification reactions. Some recent studies have suggested that gasification reactions have noticeable effects on char combustion temperature and char burning rate under conventional combustion in air [3–6]. Thus, knowledge of char gasification is also essential for improving conversion efficiency of biomass fuel particles and general energy efficiency of existing biomass/coal-fired plants. The influence of gasification reactions is even more important in oxy-fuel combustion systems, where the CO_2 levels are typically much higher than in conventional air-fired combustion and the water vapor levels can be as high as 25-34 vol-%, when employing wet flue gas recycling [5,7].

Previous studies have shown that the morphology and reactivity of char particles are sensitive to the temperature and heating rate at which they are formed [8–13]. Large-scale gasification technology, such as entrained flow gasification, often employs high temperature conversion of small fuel particles [14–17]. Therefore, in order to gain a comprehensive understanding of the process of char conversion in industrially relevant environments, similar high temperature and high heating-rate (HHR) conditions need to be employed in laboratory studies. Due to a high controllability, drop tube reactors (DTRs) are often used for this purpose, which can typically heat up pulverized solid fuel or char particles at a heating rate around 10^4 K/s to a high temperature. Various studies have been carried out to in an attempt to investigate char reactivity by directly feeding pulverized biomass into DTRs [18–21]. However, the large volatile content of biomass, and the sensitivity of the volatile yield to the particle heating rate, means that it is difficult to separate devolatilization-induced conversion from char conversion when feeding raw biomass particles into a reactor. Alternatively, char conversion can be directly investigated by separating the devolatilization process from the char conversion process. In the first step, biomass is devolatilized at high temperature and HHR in a DTR, as described in previous works [22–27]. The

Author's Post-print version. Article published in Applied Energy:
DOI: 10.1016/j.apenergy.2017.08.075
Published version: https://www.sciencedirect.com/science/article/pii/S0306261917310930

conversion behavior of the produced char is then explored at similar conditions to what the char particle is likely to experience in an actual furnace. Previous studies have employed this two-step method to investigate oxidation reactivity of coal and biomass chars in DTRs. To the authors' knowledge, very few studies on the gasification of biomass char using this two-step method in a DTR have been reported. Li et al. [28] examined the effects of torrefaction on the gasification of HHR biomass char using a DTR at 1473-1573 K. It was found that char produced from torrefied biomass had a lower reactivity than the char produced from non-torrefied biomass. Oxidation and steam gasification of several HHR chars obtained as a by-product of entrained-flow gasification were studied by Matsumoto et al. [16] using a DTR at 1173-1473 K. They found that the reactivity of investigated chars was dependent on the concentration of alkali metals in biomass feedstock and the O/C ratio in biomass char.

Despite the above-mentioned advantages, DTRs are often difficult to access with non-intrusive techniques such as optical diagnostics. Hence, char conversion is usually evaluated by first sampling via a water- or oil-cooled probe and then applying an ash/refractory element tracer technique [29,30] in most relevant studies using DTRs. Because of the inherent low ash content of biomass char, the significant release of alkali elements under high-temperature conversion conditions, and the uneven distribution of the inorganic elements in the form of different chemicals (i.e., oxides and silicates), errors may be introduced when the tracer technique is used to estimate the conversion of biomass char. In addition, the intrusive sampling probe may influence the flow and temperature field inside the DTRs, thus altering the char conversion. An alternative method is to use a combustion-driven flat-flame reactor, in which industrially relevant conditions can be realized while simultaneously employing optical diagnostics [31–38]. Valuable information, such as particle temperature, size, and velocity, can be measured during the char conversion process by employing optical pyrometry with a coded aperture. A detailed review of the analysis of the conversion of pulverized solid fuels using a lab-scale flat-flame reactor has been given by Lemaire and Menanteau [39]. Previous studies using flat-flame reactors have been primarily aimed at studying coal chars and char conversion in oxidation environments. Comprehensive investigations of the temperature of HHR biomass chars during gasification are scarce.

The primary purpose of this study is to investigate gasification behavior of HHR biomass chars at high temperatures and heating rates. To this end, the two-step method was applied where the HHR chars were produced in the DTR at 1473 K and the gasification of size-classified chars was studied in a flat-flame reactor. A non-intrusive optical particle-sizing pyrometer was used to measure time-resolved temperatures of chars in various conversion environments. The behavior of

Author's Post-print version. Article published in Applied Energy:
DOI: 10.1016/j.apenergy.2017.08.075
Published version: https://www.sciencedirect.com/science/article/pii/S0306261917310930

the investigated biomass chars was also compared to that of a common subbituminous coal char to heighten awareness of the reactivity differences between biomass-derived char and coal-derived char at elevated temperatures. This is particular important since large-scale utilization of solid biomass relies heavily on the technologies developed for coal. In addition, the experimental data has been interpreted with a comprehensive char conversion model. Kinetic parameters of the heterogeneous steam gasification reaction and Boudouard reaction were estimated for the investigated chars. A detailed sensitivity analysis was also performed using the obtained kinetic parameters to identify the most important operational parameters for the entrained-flow gasification of biomass.

2. Experimental methods

The raw biomass investigated is a forest residue consisting primarily of the tops and branches collected from Norway spruce forest. Corresponding torrefied biomass was produced in a torrefaction reactor consisting of four horizontal, electrically heated screw conveyors arranged in series [40]. In the torrefaction process, the biomass was first preheated at 498 K for 5 min and then torrefied at 548 K for 30 min. The coal examined in this study is Black Thunder, a low-sulfur subbituminous coal from the Powder River Basin in the USA. All three types of chars were produced in a 1.5 m long electrically heated DTR located at the Combustion Research Facility of Sandia National Laboratories in the USA. The wall temperatures of the DTR were maintained at 1473 K during the char production process. A bulk gas stream of 182 slpm (liters per minute at 0 °C and 1 atm) of preheated N_2 was introduced into the reactor to generate the desired pyrolysis atmosphere. The coal char was produced at the same temperature in a slightly different atmosphere, consisting of N_2 (180 slpm) with a small amount of O_2 (5.5 slpm). The details of the reactor set-up and char production process have been reported previously [22,28]. To aid data acquisition, the biomass chars were sieved to 71-90 µm and the coal char was sieved to 75-90 µm prior to investigation of char conversion. Proximate and ultimate analyses of the feedstocks and the chars are summarized in Table 1. Due to the low char yields of biomass and torrefied biomass, detailed analysis of the biomass-derived chars was not possible. Instead, only the ash contents were determined using a thermogravimetric analyzer. The biomass char contains 10.8 wt-% ash on a dry basis, whereas the torrefied biomass char contains 14.7 wt-% ash.

The gasification of chars was studied using a different reactor, namely Sandia's optical entrained flow reactor, described in detail previously [32]. As shown in Fig. 1, the combustion-driven reactor features a flat-flame reactor (diffusion-flamelet-based Hencken burner), which provides a high-temperature gas flow at ambient pressure (1 atm). The flat-flame reactor consists

Author's Post-print version. Article published in Applied Energy:
DOI: 10.1016/j.apenergy.2017.08.075
Published version: https://www.sciencedirect.com/science/article/pii/S0306261917310930

of a 46 cm tall, 5 cm by 5 cm square quartz chimney that prevents cold surrounding air from disturbing the post-combustion gas flow. Two gasification atmospheres were realized by burning mixtures of hydrogen and ethylene in oxygen diluted with N_2 or CO_2. In order to study the effect of heat of oxidization reaction on char temperature, one oxidation atmosphere was also investigated. The compositions of the post-flame gas are summarized in Table 2. The pulverized char particles were injected at the furnace centerline through a 0.75 mm stainless-steel tube. A separate, low-flow gas stream (0.03 slpm) was used to carry the char particles into the hot post-flame gas in the furnace. Depending on the diluent used in the main reactant flow, N_2 or CO_2 was chosen as the feed gas. The temperature, along with the velocity and diameter, of individual reacting char particles was measured using a particle-sizing pyrometer at different heights along the reactor centerline.

Table 1. Proximate and ultimate analysis

	Biomass	Torrefied biomass	Coal	Biomass char	Torrefied biomass char	Coal char
Proximate analysis (wt-%, as received)						
moisture	6.3	4.2	9.3	-	-	3.7
ash	2.2	2.7	4.8	-	-	9.5
volatile	70.0	61.6	42.3	-	-	12.1
fixed carbon	21.5	31.5	43.6	-	-	74.1
Ultimate analysis (wt-%, dry ash free)						
C	52.1	59.5	69.0	69.8	78.1	89.6
H	6.1	5.6	5.0	2.7	2.2	0.8
O (by diff.)	41.3	34.3	25.4	27.0	19.0	1.3
N	0.5	0.6	1.0	0.5	0.7	8.0
S	<0.02	<0.02	0.5	<0.02	<0.02	0.4

Author's Post-print version. Article published in Applied Energy:
DOI: 10.1016/j.apenergy.2017.08.075
Published version: https://www.sciencedirect.com/science/article/pii/S0306261917310930

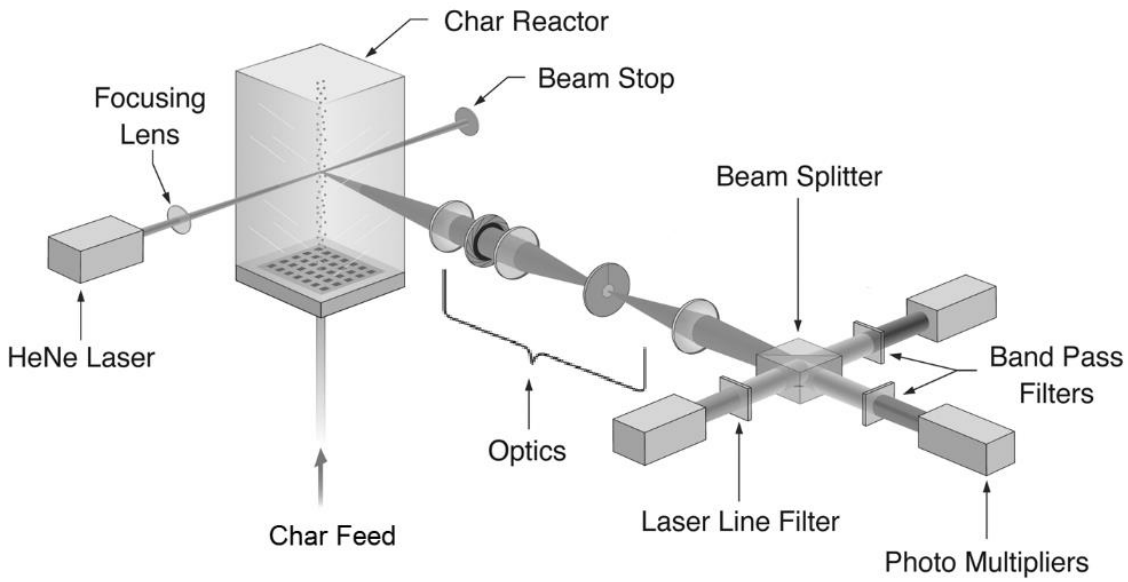

Fig. 1 Schematic of Sandia's optical entrained flow reactor [32].

Table 2. Experimental conditions

Case	Mole fractions in product gas (%)				Total product flow rate (SLPM)
	N_2	CO_2	H_2O	O_2	
1	79.7	6.4	13.9	0.0	60.0
2	0.0	86.1	13.9	0.0	57.2
3	71.1	4.0	14.3	10.6	57.4

3. Numerical analysis

To augment the interpretation of the experiments, a comprehensive char conversion model using intrinsic kinetics was applied. The model considers carbon gasification by both H_2O and CO_2. Furthermore, the model allocates the ash liberated at the particle surface to a) form an ash film, b) diffuse back into the char particle and give a dilution effect to the remaining organic fraction of the char particle, or c) act as a combination of the two effects in tandem. Fig. 2 gives a schematic illustration of the char conversion model. The initial char particle is divided into several equally spaced concentric shells. When the char particle is exposed to a reactive environment, the carbon starts to burnout and the ash in the outmost shell is then liberated. Some experimental evidence suggests that the mineral constituents exposed at pore surfaces diffuses back into the char matrix [41]. To account for this effect, a portion of the exposed ash is assumed to penetrate into the char

Author's Post-print version. Article published in Applied Energy:
DOI: 10.1016/j.apenergy.2017.08.075
Published version: https://www.sciencedirect.com/science/article/pii/S0306261917310930

core and be uniformly distributed in each of the inner shells while the remainder forms an ash film on the outside of the particle. As shown in Fig. 2, the thickness of the external ash film increases during conversion while, at the same time, the diameter of the char core shrinks. When the outmost shell (between Boundary 1 and Boundary 2) of the char core is completely burned out, the adjacent internal shell (between Boundary 2 and Boundary 3) develops a new 'outmost' shell.

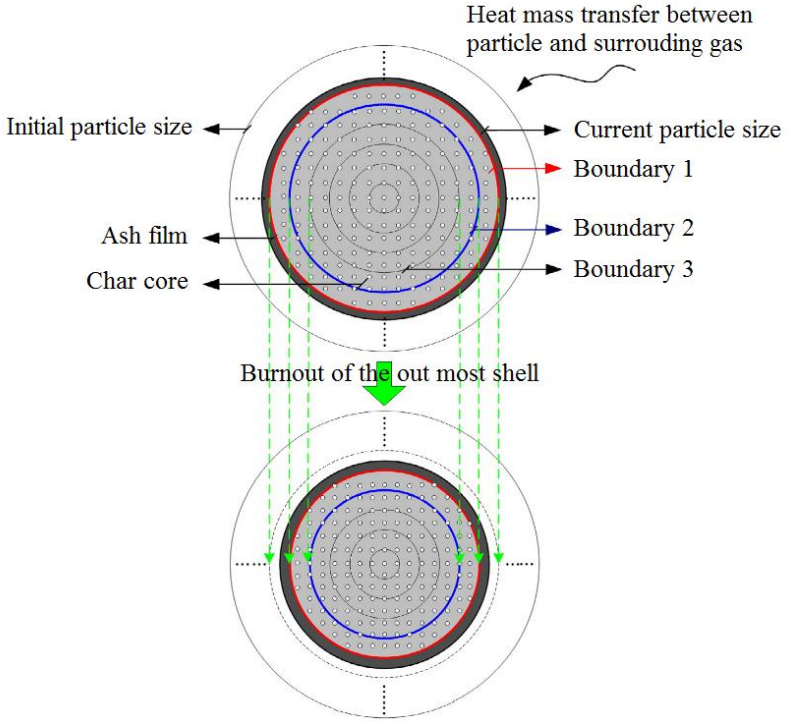

Fig. 2 Integrated ash film and ash dilution model coupled in the intrinsic char conversion model [42].

The gasification rate of char is calculated according to an intrinsic kinetics sub-model, which takes account of the effects of ash and porosity. The overall conversion rate of char, $q_{c,tot}$, consisting of the combination of the external and internal consumption of the char, is given by Eq. (1):

$$q_{c,tot} = \underbrace{(1-Y_a-\theta_c)q_{c,ex}}_{\text{external consumption of the char}} + \underbrace{(\eta\rho_c S_g d_{cc}/6)q_{c,ex}}_{\text{internal consumption of the char}} \quad (1)$$

where Y_a is the mass fraction of ash, θ_c is the porosity of carbon, η is the internal effectiveness factor, ρ_c is the density of the char, S_g is the specific internal surface area, d_{cc} is the diameter of char core, and $q_{c,ex}$ is the consumption rate per unit external surface of char core, which is calculated according to the Arrhenius expression given by Eq. (2):

Author's Post-print version. Article published in Applied Energy:
DOI: 10.1016/j.apenergy.2017.08.075
Published version: https://www.sciencedirect.com/science/article/pii/S0306261917310930

$$q_{c,ex} = A\exp(-Ea/RT)P_i^n \quad (2)$$

where A is the pre-exponential factor, Ea is the activation energy, R is the universal gas constant, T is the temperature of the char core, P_i is the partial pressure of the reactants (CO_2 or H_2O), and n is the reaction order. The first term on the right hand side of Eq. (1) accounts for the external consumption of the char, whereas the second term accounts for the internal consumption of the char by reactive gases diffusing into the char core. Considering the effects of Stefan flow and the ash film, a diffusion sub-model is used to solve for the reactant concentrations on the surface of the char and inside the char particle. The heat transfer between each ash layer is modeled through conduction, whereas the heat transfer between char and surroundings is calculated through both convection and radiation. More details about the model are available in our previous publication [42].

4. Results and discussion

4.1 Gas temperature profile

The gas temperature was measured without the presence of char particle by a 25-μm, type-R fine-wire thermocouple, and was corrected for radiant heat loss [43], as shown in Fig. 3. Due to the injection of the cold char feeding gas (0.03 slpm) in the middle of the reactor, the gas temperature below the height of 25 mm is relative low and rises quickly with increasing height (gas and particles flow upward). For gasification conditions, the gas temperature profiles of Case 1 and 2 are very similar. The temperature peaks around 1930 K and 1880 K at heights between 50 to 70 mm in Case 1 and 2, respectively. Due to heat losses via gas radiation and the unheated quartz windows, the temperature decreases with increasing height. The optical data for char particles were mainly collected between 25 and 300 mm above the burner, where the gas temperature was relatively high. Compared to the gasification cases, slightly lower temperatures were used for the oxidation Case 3, because of the fast oxidation reaction.

4.2 Measured temperature of char particles

The temperature of char particles was measured at various heights above the burner, together with the char particle velocities, from which the residence time of the char particles was determined. The measured mean particle temperatures are shown in Fig. 3 as a function of both height and residence time. The velocity differences between different types of char particles are very small, as expected for the conveyance of pulverized particles. Therefore, only one series of representative

Author's Post-print version. Article published in Applied Energy:
DOI: 10.1016/j.apenergy.2017.08.075
Published version: https://www.sciencedirect.com/science/article/pii/S0306261917310930

residence time is given in each condition. One should note that every temperature shown in Fig. 3 is an average of temperatures that were measured from at least 100 char particles. As discussed by Murphy and Shaddix [32], the precision of the single-particle measurement is estimated to be better than ± 1%. In the current study, the standard error of the mean is typically less than 10 K. As a result, the sample standard deviation can be estimated within 100 K under all investigated conditions. Considering that the measured char temperature is in the range of 1500 to 1900 K, the spread in the mean char temperatures is relatively small. More comprehensive analyses of the accuracy and error of these measurements can be found elsewhere [32,44].

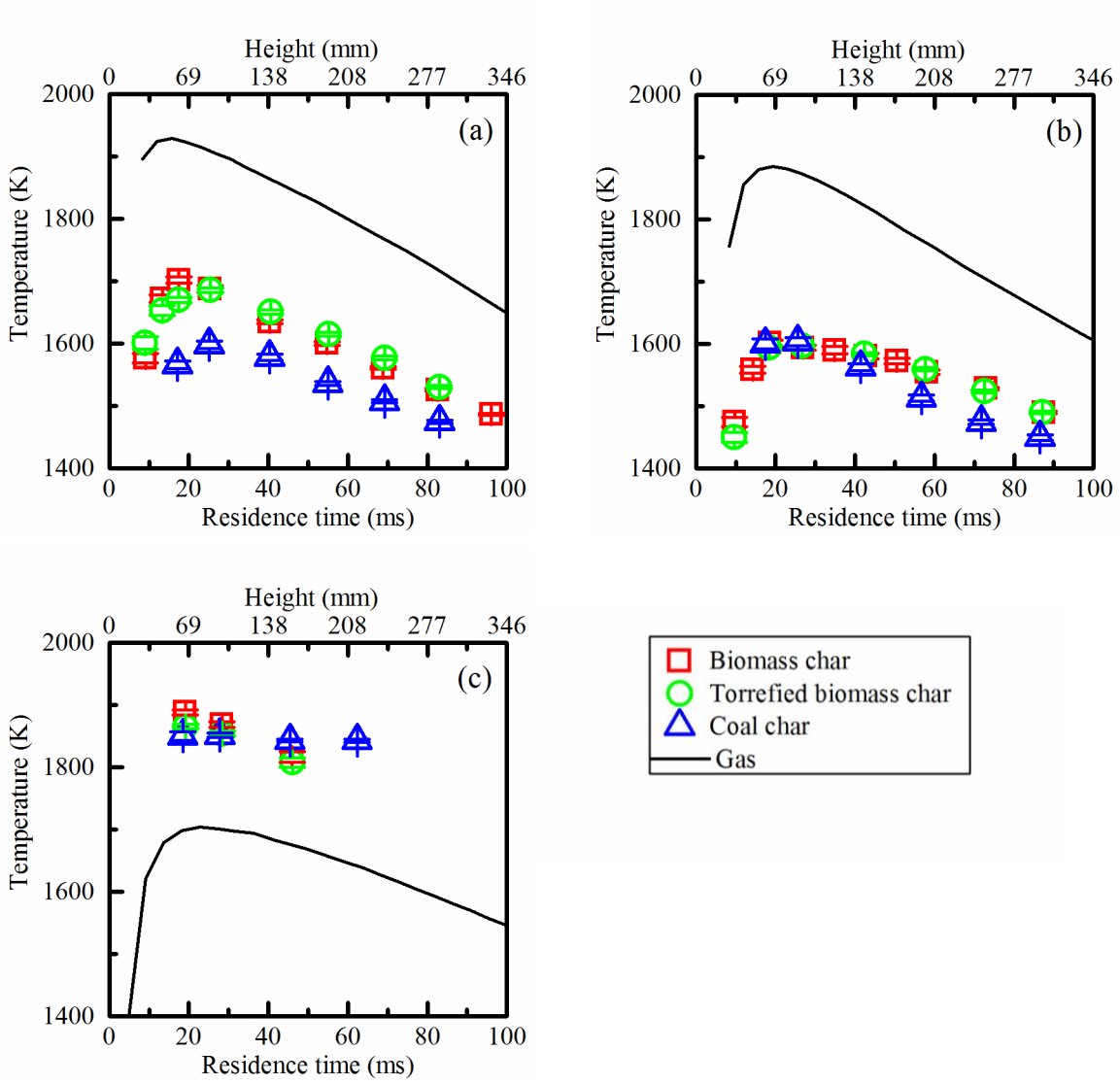

Fig. 3 Measured temperatures of char particles under different atmospheres. The error bar is the range of plus/minus one standard error of the mean. (a) Case 1: Gasification, 79.7% N_2, 13.9%

Author's Post-print version. Article published in Applied Energy:
DOI: 10.1016/j.apenergy.2017.08.075
Published version: https://www.sciencedirect.com/science/article/pii/S0306261917310930

H_2O, and 6.4% CO_2; (b) Case 2: Gasification, 13.9% H_2O, and 86.1% CO_2; (c) Case 3: Oxidation, 71.1% N_2, 14.3% H_2O, 4.0% CO_2, and 10.6% O_2.

At both gasification conditions, all the investigated chars show similar temperature profiles. The temperature of the char particles first increases when the char is fed into the reactor, and then the temperature slowly decreases, following the general trajectory of the gas temperature. It is noteworthy that the char particle temperature is substantially lower than the temperature of the surrounding gas under gasification conditions, which can be attributed to the combined effects of radiant heat losses to cooler lab surroundings and endothermic char reactions. Carbon-rich chars have been measured to have a radiant emissivity of approximately 0.80, independent of temperature [45]. Although the investigated chars may have somewhat different emissivities due to variations in carbon and ash content, the differences can generally be assumed to be small. Therefore, the radiant losses from all of the different chars are expected to be very close. In fact, the endothermic heat of reaction plays a more important role on the temperature deficit of the char particles relative to the surrounding gas than radiant loss, as our calculations show (below).

Fig. 3(c) shows that the temperature of the char particles is clearly higher than the gas temperature when burning in the presence of oxygen, due to the exothermic char oxidation reaction (ΔH = -110.62 kJ/mol for $C+0.5O_2 \rightarrow CO$ and ΔH = -393.77 kJ/mol for$C+O_2 \rightarrow CO_2$). This also implies that the low temperature of char particles in Figs. 3(a) and 3(b) is caused primarily by the endothermic steam gasification reaction (ΔH = 131.38 kJ/mol carbon) and Boudouard reaction (ΔH = 172.58 kJ/mol carbon). As a result, the difference in temperature between the char particle and the surrounding gas can be viewed as an indication of char reactivity. In general, lower char particle temperature correlates with higher gasification reactivity under gasification conditions.

It can be seen from Figs. 3(a) and 3(b) that there are no significant differences in the mean temperature of the two biomass chars, suggesting a similar gasification reactivity. It is interesting to note that the same torrefied biomass char source showed a lower CO_2 reactivity than the raw biomass char at a gas temperature of 1573 K in a previous study [28]. One major difference between the two studies is the size of the investigated char particles. In the current study, the chars were sieved into a narrow size fraction (71-90 μm), whereas in the previous study the chars were kept in their original form with wide size distributions. In particular, the volume-mean size of the torrefied biomass char particles in the previous study was significantly larger than that of the raw biomass char. Several potential explanations were raised in the previous study to explain the effects of

Author's Post-print version. Article published in Applied Energy:
DOI: 10.1016/j.apenergy.2017.08.075
Published version: https://www.sciencedirect.com/science/article/pii/S0306261917310930

torrefaction on high temperature reactivity of high heating rate chars. Based on the results from the current study, it can be concluded that the differences in char particle size probably accounted for the reactivity differences seen in the previous study.

Compared to the biomass chars, the temperature of the coal char is relatively low under both gasification conditions, implying a higher gasification reactivity of the coal char than the two biomass chars. This may seem counterintuitive since it is often believed that biomass char inherently has higher reactivity than coal char and at low temperatures the alkali content of biomass helps to catalyze oxidation and gasification reactions. However, experimental studies of the high temperature reactivity of biomass chars are very rare [46], and the research that has been reported has generally found biomass chars to have similar high temperature oxidation reactivity as low- to mid-rank coal chars [47]. In fact, a recent study [33] reported that corn stover char has a much lower reactivity towards steam than Wyodak subbituminous coal char. Several possible explanations were proposed by the authors, such as the intrinsic differences between the carbonaceous surfaces of the biomass and coal chars and different intensity of gasification inhibition by CO and H_2. A major difference between biomass chars and coal chars is the high oxygen content of biomass chars, which persists during char conversion [28,48]. This difference in the chemical structure of the char likely influences its reactivity and also has implications for interpreting measurements of char particle temperatures in terms of particle reactivity (owing to differences in the reaction enthalpy of reactions involving the oxidation or gasification of char carbon). A recent study using computational quantum chemistry showed that CO_2 desorption from char surfaces with embedded oxygen is more difficult, suggesting a potential chemical mechanism for lower reactivity of biomass chars [49]. Similar effects may also be expected for the gasification process. More detailed characterization of different types of biomass char is needed to link biomass char reactivity with physico-chemical properties. In addition, different approaches including quantum chemistry calculations of char energy states should be applied to clarify key factors that affect char reactivities.

Since biomass has a much higher volatile content than coal, it is generally assumed that the reactivity of biomass during gasification is much higher than that of coal [50]. However, based on the measurements in this study the complete gasification of biomass feedstocks may require similar times compared to that of coal in industrial applications, especially considering that relatively large biomass fuel particles are often used.

4.3 Simulated temperature of char particles

Author's Post-print version. Article published in Applied Energy:
DOI: 10.1016/j.apenergy.2017.08.075
Published version: https://www.sciencedirect.com/science/article/pii/S0306261917310930

An analysis of the intrinsic kinetic parameters of the gasification reactions was conducted using the char conversion model outlined in Section 3. Due to the similar temperature profiles found for the raw biomass char and the torrefied biomass char, the model parameters of both types of biomass chars were considered the same in this numerical study. Based on the current experimental data and previous studies [16,42,51] performed under similar conditions, the initial values of d_{cc} and ρ_c were assumed to be 85 μm and 250 kg /m^3 for biomass char, and 90 μm and 550 kg/m^3 for coal char, respectively. In addition, the initial value of S_g was set to be 247 m^2/g for both biomass and coal char, whereas the intrinsic reaction orders of both the steam gasification reaction and the Boudouard reaction were fixed at 0.5. Furthermore, according to the suggestions given by Hecht et al. [3,5], acceptable activation energies were limited to the range of 190-251 kJ/mol. Since the pre-exponential factor is highly dependent on the activation energy used, as well as the fuel type and char-formation conditions, it was empirically fit to the experimental results. The best-fit kinetic parameters are listed in Table 3. The principal interest of this study is the gasification behavior. Therefore, only the data from the gasification reaction conditions were used to obtain kinetic parameters.

Table 3. Kinetic parameters

Char	Steam gasification reaction		Boudouard reaction	
	Pre-exponential factor g/s/cm^2/atm$^{0.5}$	Activation energy kJ/mol	Pre-exponential factor g/s/cm^2/atm$^{0.5}$	Activation energy kJ/mol
Biomass	2.0×10^4	190	5.0×10^4	210
Coal	8.0×10^4	190	1.0×10^5	251

Fig. 4 presents a comparison of the measured mean char particle temperatures and the simulated temperatures of the char particles using the best-fit kinetic parameters. It can be observed that the simulated results are quite close to the measured data for both investigated conditions, Case 1 and 2. The model can predict nearly all the measured data within only ±5% error bands. Moreover, similar to our previous work [42], the model can well capture the char particle temperature profile along the centerline of the furnace. It was found that activation energies of 222 kJ/mol for steam gasification and 251 kJ/mol for the Boudouard reaction gave the best agreement between the

Author's Post-print version. Article published in Applied Energy:
DOI: 10.1016/j.apenergy.2017.08.075
Published version: https://www.sciencedirect.com/science/article/pii/S0306261917310930

measured coal char particle temperatures and modeling results when using an apparent kinetics model in a previous investigation [4]. However, it is impossible to reproduce the observed coal char temperatures in this study by using the suggested activation energies in an intrinsic kinetics model. Instead, a lower activation energy for steam gasification (190 kJ/mol) has been obtained here. It is also worth noting that a smaller pre-exponential factor for steam gasification reaction was found for biomass char than for coal char, which is in agreement with the reported experimental evidence [33], as mentioned in the previous section.

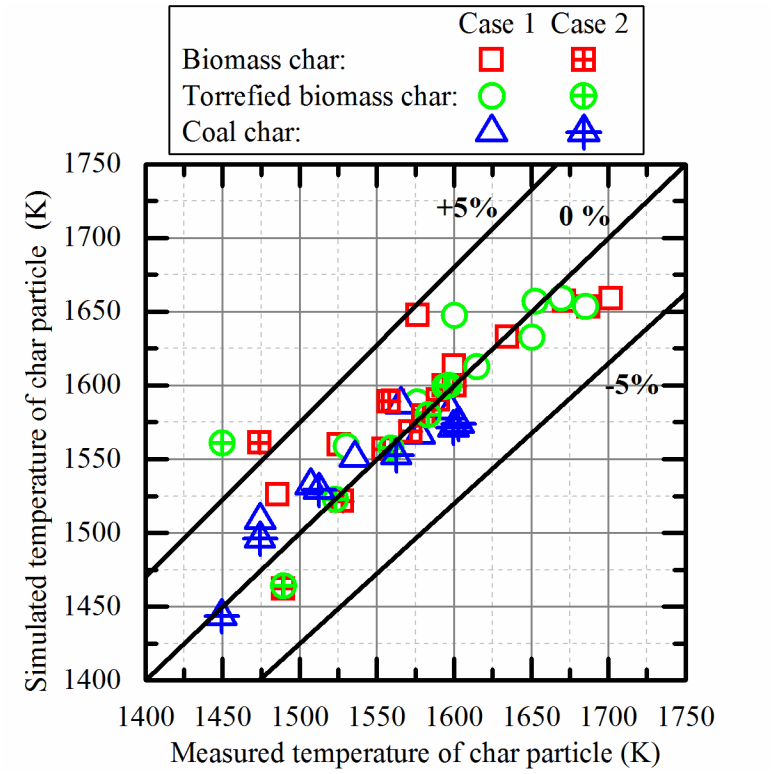

Fig.4 Comparison of simulated char particle temperature and measured char particle temperature. The solid lines correspond to the deviations of +5%, 0%, and -5%.

4.4 Sensitivity analysis

Since gasification conditions may vary considerably, it is of interest to investigate the sensitivity of the gasification behavior of biomass-derived char to operational parameters. As shown in Table 4, a reference condition for char gasification was estimated first according to an experiment reported in the literature, where wood powder was gasified in an oxygen-blown entrained-flow reactor [17]. The concentrations of CO_2 and H_2O used in this calculation were

Author's Post-print version. Article published in Applied Energy:
DOI: 10.1016/j.apenergy.2017.08.075
Published version: https://www.sciencedirect.com/science/article/pii/S0306261917310930

determined based on the experimental operating condition of a fuel/oxygen equivalence ratio of 2.0. Other gas components found in a gasifier, such as H_2, CO, and CH_4, were replaced by N_2 for simplicity. The oxygen-blown entrained-flow reactor is typically designed to work in a slagging mode. Hence, a relatively high temperature of 1573 K has been chosen for analysis. Fig. 5 shows the profiles of carbon conversion and char temperature calculated at the reference condition using the char conversion model with the kinetic parameters listed in Table 3 for the biomass chars. Consistent with the results shown previously, the char temperature is always lower than the gas temperature. The entire conversion process takes 0.39s (time used for reaching carbon conversion ratio of 99%), which is of the same magnitude as the previous study where high-heating rate biomass-derived chars were gasified under similar conditions [28].

Table 4. Reference condition of char gasification

Char properties		Gas composition			Temperature
Diameter (μm)	Density (kg/m^3)	CO_2 (vol-%)	H_2O (vol-%)	N_2 (vol-%)	(K)
100	250	15	15	70	1573

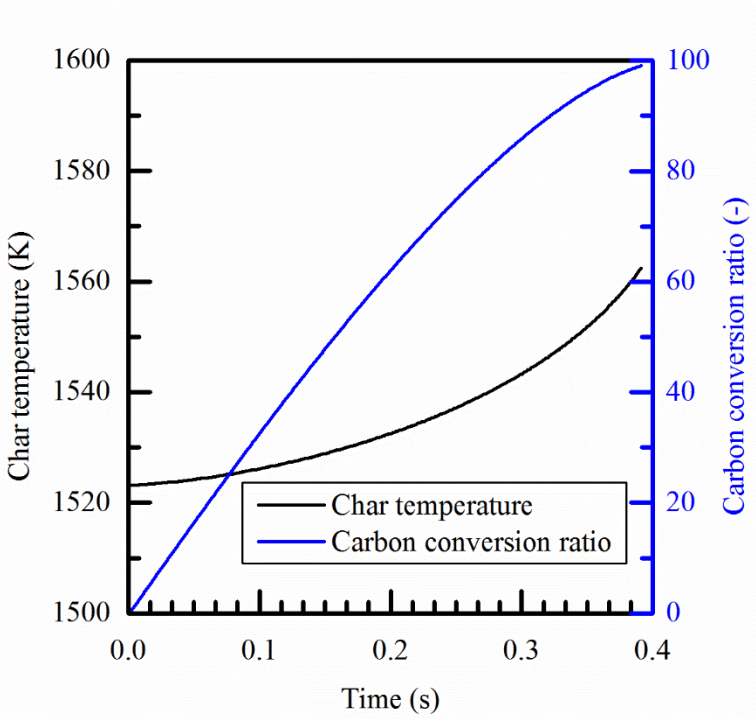

Fig. 5 Prediction of biomass char carbon conversion ratio and char temperature at the reference condition.

Author's Post-print version. Article published in Applied Energy:
DOI: 10.1016/j.apenergy.2017.08.075
Published version: https://www.sciencedirect.com/science/article/pii/S0306261917310930

Four parameters, including the gas temperature, char density, char diameter, and steam concentration, were selected to investigate their effects on char gasification. By varying the parameters accordingly, the carbon conversion time (time used for reaching carbon conversion ratio of 99%) in each case was compared to the conversion time obtained at the reference condition, as shown in Fig. 6. With respect to variation of the absolute value of a variable, gas temperature is clearly the most influential factor on char conversion for the investigated conditions. In an industrial oxygen-blown entrained-flow gasifier, the process temperature is maintained by partially combusting the fuel. However, due to the inherent non-uniformity of biomass and uneven fuel-feeding rate, the temperature inside the gasifier may also vary in time, potentially causing a large fluctuation in carbon conversion and composition of the product gas. Under the investigated conditions, variations in the char density and char diameter have a minor effect on char gasification. Nevertheless, many factors may influence the char density and char diameter in the practical operation of biomass gasification. For instance, biomass containing higher volatile content tends to produce char with lower density. Because they are limited to short residence times, entrained-flow gasifiers can only operate with relatively small fuel particles. Therefore, torrefaction, an effective pretreatment that can significantly improve the grindability of biomass, is often required for gasification of lignocellulosic biomass. As mentioned previously, the size distribution can however be very different between char produced from torrefied biomass and char produced from non-torrefied biomass [28]. As a result, a different characteristic char gasification time may be expected by using torrefied and non-torrefied biomass, even when the feedstocks are sieved to the same size range.

Author's Post-print version. Article published in Applied Energy:
DOI: 10.1016/j.apenergy.2017.08.075
Published version: https://www.sciencedirect.com/science/article/pii/S0306261917310930

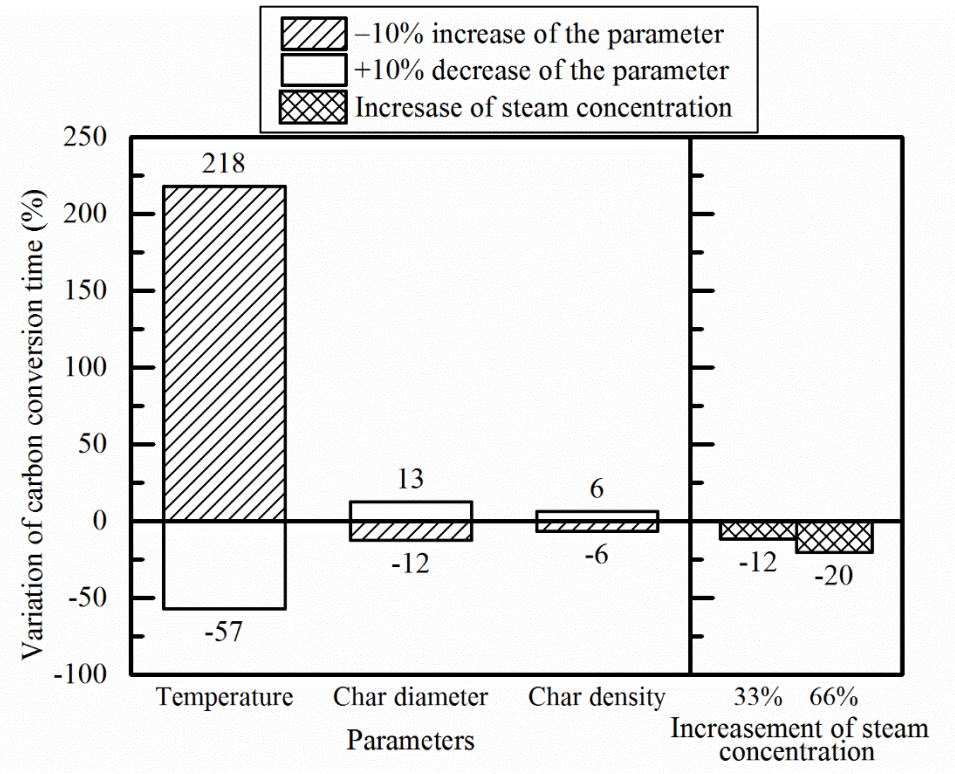

Fig. 6 Sensitivity analysis of the operational parameters.

Finally, the effect of steam concentration in the reactor was studied, as steam is another common gasification agent for entrained-flow gasification. The H_2 to CO ratio of the syngas can be increased by using a mixture of oxygen and steam in the gasification process. This is particularly attractive for biomass-to-liquid application using the Fischer–Tropsch fuel-synthesis process. The sensitive analysis of steam on char gasification was carried out by changing the composition of the gas mixture. The concentration of steam was increased by 33% and 66%, which roughly correspond to oxygen-steam molar ratios of 2:1 and 1:1. The resulting volume fractions are H_2O=0.20, CO_2=0.14, N_2=0.66, and H_2O=0.25, CO_2=0.13, N_2=0.62, respectively. It is shown in Fig. 6 that the carbon conversion time is lower when the steam concentration is increased. This phenomenon is mainly attributed to the fact that the steam reaction rate is much faster than the rate of the Boudouard reaction under the investigated conditions.

5. Conclusion

In order to investigate the gasification behavior of high-heating rate chars at elevated temperatures, two biomass-derived chars and one subbituminous coal char produced at high-heating rates were investigated in an optical entrained flow reactor. Char particle temperatures and

Author's Post-print version. Article published in Applied Energy:
DOI: 10.1016/j.apenergy.2017.08.075
Published version: https://www.sciencedirect.com/science/article/pii/S0306261917310930

the surrounding gas temperature in three different gas mixtures were measured with high accuracy, providing essential time-resolved data for model development and validation. Regardless of the gasification conditions, char particles produced from torrefied and non-torrefied biomass were found to have very similar temperatures during their conversion process, suggesting that torrefaction has a minor effect on reactivity of char at high temperature. In conjunction with previous studies, the effects of torrefaction treatment of raw biomass on conversion behavior of char is primarily attributed to differences in char particle size. Surprisingly, the tested high-heating rate coal char exhibits a lower temperature than the tested biomass chars for both investigated gasification conditions, suggesting a higher gasification reactivity for the coal char. The measured char particle temperatures were interpreted with a comprehensive char conversion model using intrinsic kinetics. The kinetic parameters of the steam gasification reaction and Boudouard reaction were determined with an intrinsic reaction order of 0.5, which was shown to yield reasonably accurate char particle temperature predictions. Using the obtained kinetic parameters, a sensitive analysis at a typical condition of oxygen blown entrained-flow gasification reveals that gas temperature has a more dominant effect on carbon conversion time than the diameter and density of the char particle.

Acknowledgements

This publication has been funded by CenBio–Norwegian Bioenergy Innovation Centre and the National Nature Science Foundation of China (Grant Number 51406149). CenBio is co-funded by the Research Council of Norway (193817/E20) under the FME scheme and the research and industry partners. Special thanks to Manfred Geier for his assistance with the experiments at Sandia National Laboratories. Sandia National Laboratories is a multiprogram laboratory operated by Sandia Corporation, a Lockheed Martin Company, for the US Department of Energy under contract DE-AC04-94-AL85000.

Reference

[1] K.P. de Jong, Surprised by selectivity, Science. 351 (2016) 1030–1031.

[2] J. Andersson, J. Lundgren, Techno-economic analysis of ammonia production via integrated biomass gasification, Appl. Energy. 130 (2014) 484–490.

[3] E.S. Hecht, C.R. Shaddix, A. Molina, B.S. Haynes, Effect of CO_2 gasification reaction on oxy-combustion of pulverized coal char, Proc. Combust. Inst. 33 (2011) 1699–1706.

[4] M. Geier, C.R. Shaddix, K. A. Davis, H.-S. Shim, On the use of single-film models to describe the oxy-fuel combustion of pulverized coal char, Appl. Energy. 93 (2012) 675–

Author's Post-print version. Article published in Applied Energy:
DOI: 10.1016/j.apenergy.2017.08.075
Published version: https://www.sciencedirect.com/science/article/pii/S0306261917310930

679.

[5] E.S. Hecht, C.R. Shaddix, M. Geier, A. Molina, B.S. Haynes, Effect of CO_2 and steam gasification reactions on the oxy-combustion of pulverized coal char, Combust. Flame. 159 (2012) 3437–3447.

[6] C. Gonzalo-Tirado, S. Jiménez, J. Ballester, Gasification of a pulverized sub-bituminous coal in CO_2 at atmospheric pressure in an entrained flow reactor, Combust. Flame. 159 (2012) 385–395.

[7] Y. Tan, Oxy-fuel combustion for power generation and carbon dioxide (CO_2) capture, Woodhead Publishing, 2011.

[8] C. Di Blasi, Combustion and gasification rates of lignocellulosic chars, Prog. Energy Combust. Sci. 35 (2009) 121–140.

[9] M. Guerrero, M.P. Ruiz, M.U. Alzueta, R. Bilbao, A. Millera, Pyrolysis of eucalyptus at different heating rates: studies of char characterization and oxidative reactivity, J. Anal. Appl. Pyrolysis. 74 (2005) 307–314.

[10] C. Fushimi, K. Araki, Y. Yamaguchi, A. Tsutsumi, Effect of heating rate on steam gasification of biomass. 1. Reactivity of char, Ind. Eng. Chem. Res. 42 (2003) 3922–3928.

[11] E. Cetin, R. Gupta, B. Moghtaderi, Effect of pyrolysis pressure and heating rate on radiata pine char structure and apparent gasification reactivity, Fuel. 84 (2005) 1328–1334.

[12] K. Whitty, R. Backman, M. Hupa, Influence of char formation conditions on pressurized black liquor gasification rates, Carbon N. Y. 36 (1998) 1683–1692.

[13] R. Xiao, X. Chen, F. Wang, G. Yu, Pyrolysis pretreatment of biomass for entrained-flow gasification, Appl. Energy. 87 (2010) 149–155.

[14] A. Tremel, T. Haselsteiner, C. Kunze, H. Spliethoff, Experimental investigation of high temperature and high pressure coal gasification, Appl. Energy. 92 (2012) 279–285.

[15] S. Xu, Y. Ren, B. Wang, Y. Xu, L. Chen, X. Wang, T. Xiao, Development of a novel 2-stage entrained flow coal dry powder gasifier, Appl. Energy. 113 (2014) 318–323.

[16] K. Matsumoto, K. Takeno, T. Ichinose, T. Ogi, M. Nakanishi, Gasification reaction kinetics on biomass char obtained as a by-product of gasification in an entrained-flow gasifier with steam and oxygen at 900–1000°C, Fuel. 88 (2009) 519–527.

[17] F. Weiland, H. Hedman, M. Marklund, H. Wiinikka, O. Öhrman, R. Gebart, Pressurized oxygen blown entrained-flow gasification of wood powder, Energy & Fuels. 27 (2013) 932–941.

[18] S. Pereira, P.C.R. Martins, M. Costa, Kinetics of poplar short rotation coppice obtained from thermogravimetric and drop tube furnace experiments, Energy & Fuels. 30 (2016) 6525–6536.

[19] J.G. Pohlmann, E. Osório, A.C.F. Vilela, M.A. Diez, A.G. Borrego, Pulverized combustion under conventional (O_2/N_2) and oxy-fuel (O_2/CO_2) conditions of biomasses treated at different temperatures, Fuel Process. Technol. 155 (2017) 174–182.

[20] O. Karlström, A. Brink, E. Biagini, M. Hupa, L. Tognotti, Comparing reaction orders of anthracite chars with bituminous coal chars at high temperature oxidation conditions, Proc. Combust. Inst. 34 (2013) 2427–2434.

Author's Post-print version. Article published in Applied Energy:
DOI: 10.1016/j.apenergy.2017.08.075
Published version: https://www.sciencedirect.com/science/article/pii/S0306261917310930

[21] A.W. Palumbo, J.C. Sorli, A.W. Weimer, High temperature thermochemical processing of biomass and methane for high conversion and selectivity to H_2-enriched syngas, Appl. Energy. 157 (2015) 13–24.

[22] T. Li, L. Wang, X. Ku, B.M. Güell, T. Løvås, C.R. Shaddix, Experimental and modeling study of the effect of torrefaction on the rapid devolatilization of biomass, Energy & Fuels. 29 (2015) 4328–4338.

[23] A. Trubetskaya, P.A. Jensen, A.D. Jensen, A.D. Garcia Llamas, K. Umeki, P. Glarborg, Effect of fast pyrolysis conditions on biomass solid residues at high temperatures, Fuel Process. Technol. 143 (2016) 118–129.

[24] H. Lu, W. Robert, G. Peirce, B. Ripa, L.L. Baxter, Comprehensive study of Biomass particle combustion, Energy & Fuels. 22 (2008) 2826–2839.

[25] S. Septien, S. Valin, M. Peyrot, C. Dupont, S. Salvador, Characterization of char and soot from millimetric wood particles pyrolysis in a drop tube reactor between 800°C and 1400°C, Fuel. 121 (2014) 216–224.

[26] P. McNamee, L.I. Darvell, J.M. Jones, A. Williams, The combustion characteristics of high-heating-rate chars from untreated and torrefied biomass fuels, Biomass and Bioenergy. 82 (2015) 63–72.

[27] J. Li, G. Bonvicini, E. Biagini, W. Yang, L. Tognotti, Characterization of high-temperature rapid char oxidation of raw and torrefied biomass fuels, Fuel. 143 (2015) 492–498.

[28] T. Li, M. Geier, L. Wang, X. Ku, B.M. Güell, T. Løvås, C.R. Shaddix, Effect of torrefaction on physical properties and conversion behavior of high heating rate char of forest residue, Energy & Fuels. 29 (2015) 177–184.

[29] P.M. Hald, Ash tracer technique,Forskningscenter Risø, Denmark, 1995.

[30] R. Pace, P. Hedman, L. Smoot, Titanium as a tracer for determining coal burnout, American Chemical Society annual meeting, Las Vegas, NV (US), 1982.

[31] Y. Yuan, S. Li, G. Li, N. Wu, Q. Yao, The transition of heterogeneous-homogeneous ignitions of dispersed coal particle streams, Combust. Flame. 161 (2014) 2458–2468.

[32] J.J. Murphy, C.R. Shaddix, Combustion kinetics of coal chars in oxygen-enriched environments, Combust. Flame. 144 (2006) 710–729.

[33] M.B. Tilghman, R.E. Mitchell, Coal and biomass char reactivities in gasification and combustion environments, Combust. Flame. 162 (2015) 3220–3235.

[34] M. Schiemann, N. Vorobiev, V. Scherer, A Stereoscopic Pyrometer for Char Combustion Characterization, Appl. Opt. 54 (2015) 1097–1108.

[35] T.K. Gale, C.H. Bartholomew, T.H. Fletcher, Decreases in the swelling and porosity of bituminous coals during devolatilization at high heating rates, Combust. Flame. 100 (1995) 94–100.

[36] F. Carbone, F. Beretta, A. D'Anna, A flat premixed flame reactor to study nano-ash formation during high temperature pulverized coal combustion and oxygen firing, Fuel. 90 (2011) 369–375.

[37] E. Therssen, L. Gourichon, L. Delfosse, Devolatilization of coal particles in a flat flame-experimental and modeling study, Combust. Flame. 103 (1995) 115–128.

Author's Post-print version. Article published in Applied Energy:
DOI: 10.1016/j.apenergy.2017.08.075
Published version: https://www.sciencedirect.com/science/article/pii/S0306261917310930

[38] J.M. Johansen, R. Gadsbøll, J. Thomsen, P.A. Jensen, P. Glarborg, P. Ek, N.D. Martini, M. Mancini, R. Weber, R.E. Mitchell, Devolatilization kinetics of woody biomass at short residence times and high heating rates and peak temperatures, Appl. Energy. 162 (2016) 245–256.

[39] R. Lemaire, S. Menanteau, Development and numerical/experimental characterization of a lab-scale flat flame reactor allowing the analysis of pulverized solid fuel devolatilization and oxidation at high heating rates, Rev. Sci. Instrum. 87 (2016) 15104.

[40] R.A. Khalil, Q. Bach, Ø. Skreiberg, K. Tran, Performance of a Residential Pellet Combustor Operating on Raw and Torrefied Spruce and Spruce-Derived Residues, Energy & Fuels. 27 (2013) 4760–4769.

[41] M.M. Lunden, N.Y.C. Yang, T.J. Headley, C.R. Shaddix, Mineral-char interactions during char combustion of a high-volatile coal, Symp. Combust. 27 (1998) 1695–1702.

[42] Y. Niu, C.R. Shaddix, A sophisticated model to predict ash inhibition during combustion of pulverized char particles, Proc. Combust. Inst. 35 (2015) 561–569.

[43] C.R. Shaddix, Correcting Thermocouple Measurements for Radiation Loss: A Critical Review, in: M. Jensen, M.K.; Di Marzo (Ed.), Proc. 33rd Natl. Heat Transf. Conf. NHTC'99, Albuquerque, NM (US), 1999.

[44] D. Tichenor, R.E. Mitchell, K.R. Hencken, S. Niksa, Simultaneous in situ measurement of the size, temperature and velocity of particles in a combustion environment, Symp. Combust. 20 (1985) 1213–1221.

[45] P.R. Solomon, R.M. Carangelo, P.E. Best, J.R. Markham, D.G. Hamblen, The spectral emittance of pulverized coal and char, Symp. Combust. 21 (1988) 437–446.

[46] A. Williams, M. Pourkashanian, J.M. Jones, Combustion of pulverised coal and biomass, Prog. Energy Combust. Sci. 27 (2001) 587–610.

[47] M.J. Wornat, R.H. Hurt, K. a. Davis, N.Y.C. Yang, Single-particle combustion of two biomass chars, Symp. Combust. 26 (1996) 3075–3083.

[48] M.J. Wornat, R.H. Hurt, N.Y.C. Yang, T.J. Headley, Structural and compositional transformations of biomass chars during combustion, Combust. Flame. 100 (1995) 131–143.

[49] F. Vallejos-Burgos, N. Díaz-Pérez, Á. Silva-Villalobos, R. Jiménez, X. García, L.R. Radovic, On the structural and reactivity differences between biomass- and coal-derived chars, Carbon N. Y. 109 (2016) 253–263.

[50] A. van der Drift, H. Boerrigter, B. Coda, M.K. Cieplik, K. Hemmes, Entrained flow gasification of biomass, ECN, Netherlands, 2004.

[51] E.S. Hecht, C.R. Shaddix, J.S. Lighty, Analysis of the errors associated with typical pulverized coal char combustion modeling assumptions for oxy-fuel combustion, Combust. Flame. 160 (2013) 1499–1509.